Available online at www.sciencedirect.com
ScienceDirect
Trans. Nonferrous Met. Soc. China 20(2010) 1936−1943
Transactions of Nonferrous Metals Society of China
www.tnmsc.cn

Corrosion behavior of Mg-Al-Pb and Mg-Al-Pb-Zn-Mn alloys in 3.5% NaCl solution

WANG Nai-guang(王乃光)[1], WANG Ri-chu(王日初)[1], PENG Chao-qun(彭超群)[1], FENG Yan(冯 艳)[1], ZHANG Xiang-yu(张翔宇)[2]

1. School of Materials Science and Engineering, Central South University, Changsha 410083, China;
2. Changsha Research Institute of Mining and Metallurgy, Changsha 410012, China

Received 25 August 2009; accepted 28 January 2010

Abstract: Mg-6%Al-5%Pb and Mg-6%Al-5%Pb-0.55%Zn-0.22%Mn (mass fraction) alloys were prepared by induction melting with the protection of argon. The corrosion behaviors of these alloys were studied by electrochemical measurements and immersion tests. The results show that at the corrosion onset of Mg-Al-Pb anode there is an incubation period that can be shortened with 0.55%Zn and 0.22%Mn additions in the magnesium matrix. The corrosion rate of Mg-Al-Pb anode is mainly determined by the incubation period. Short incubation period always leads to high corrosion rate while long incubation period leads to low corrosion rate. The corrosion rates based on the corrosion current density by the electrochemical measurements do not agree with the measurements evaluated from the evolved hydrogen volume.

Key words: magnesium anode; AP65 Mg alloy; corrosion resistance; hydrogen evolution; electrochemistry

1 Introduction

Because of the rapid activation, high cell voltage, wide voltage range, high power density capability, relatively low density, low electrode potential and long unactivated storage life[1−4], magnesium alloys have been developed as anode materials used in seawater battery system and cathodic protection such as in sonobuoys, beacons, emergency equipment, balloon batteries and life jackets[5−8]. However, a critical limitation for the service of magnesium anodes is their susceptibility to corrosion[9−11].

The corrosion process of magnesium anodes is mainly controlled by the composition of the α-Mg matrix, the volume fraction and the morphology of the second phase[12−13]. AP65 Mg alloy is one of these magnesium anodes with the nominal composition of 6% Al, 5% Pb (mass fraction) and balance Mg. It is reported that aluminium, added into the magnesium matrix, can enhance the corrosion resistance of magnesium alloy in NaCl aqueous solution[12−15]. It has also been demonstrated that the corrosion resistance of magnesium alloy can be improved with lead in the magnesium matrix[16]. UDHAYAN et al[17] studied the corrosion behavior of AP65 in various concentrations of magnesium perchlorate solutions and found that its electrode/electrolyte interfacial process is determined by an activation-controlled reaction. CAO et al[4] studied the electrochemical oxidation behaviors of Mg-Li-Al-Ce-Zn and Mg-Li-Al-Ce-Zn-Mn anodes in NaCl aqueous solution and found that zinc and manganese can improve the electrochemical activity of magnesium anode. Besides, manganese prevented the formation of dense oxide film on the alloy surface and facilitated peeling off of the oxidation products. But so far, there are few reports about the corrosion behavior of AP65 in NaCl aqueous solution with zinc and manganese in the magnesium matrix and its behavior of hydrogen evolution is not clearly understood. The aim of this work is to study the corrosion behavior of AP65 immersed in NaCl aqueous solution with and without a small quantity of zinc and manganese in the magnesium matrix.

2 Experimental

Mg-6%Al-5%Pb and Mg-6%Al-5%Pb-0.55%Zn-0.22%Mn alloys (mass fraction) were prepared by ingots

Foundation item: Project(JPPT-115-168) supported by National Key Science and Technological Project of China
Corresponding author: WANG Ri-chu; Tel: +86-731-88836638; Fax: +86-731-88836638; E-mail: wrc@mail.csu.edu.cn
DOI: 10.1016/S1003-6326(09)60398-8

of pure magnesium (99.99%), pure aluminium (99.99%), pure lead (99.99%), pure zinc (99.99%) and Mg-22%Mn (mass fraction) alloy by induction melting at 750 ºC with the protection of argon. The molten metals were poured into a stainless steel mold and cooled down to ambient temperature under argon atmosphere. The magnesium anode specimens were cut from the magnesium alloy ingots, homogenized at 400 ºC for 24 h, water quenched (in order to obtain the solid solutions) and aged at 200 ºC and 100 ºC for 8 h, respectively. All these heat treatment processes were performed under argon atmosphere. The microstructures of the magnesium anode specimens were examined by scanning electron microscopy (SEM) after preparation by mechanical grinding successively to 1 000 grit SiC paper, polishing successively to 0.5 μm diamond, washing and drying.

Potentiodynamic polarization curves and open circuit potential curves were measured by IM6ex potentiostat with a standard three-electrode glass cell. Each measurement started immediately after the specimen was immersed in 3.5% (mass fraction) NaCl aqueous solution at 25 ºC. The electrolyte solution was made with analytical grade reagents and deionized water. Open circuit potential curves were obtained at the current density of zero and potentiodynamic polarization curves were obtained at a scan rate of 2 mV/s. Each specimen for the electrochemical measurement was encapsulated in epoxy resin with a surface of 10 mm×10 mm exposed to NaCl aqueous solution. The specimen surface was ground successively to 1 000 grit SiC paper. A platinum gauze was used as the counter electrode and a saturated calomel electrode (SCE) as the reference electrode. All potentials were referred to the SCE.

The corrosion behavior of the magnesium anodes was also researched by immersion tests during which the specimens were immersed in 3.5% NaCl (mass fraction) solution at 25 ºC for 13 h. Each specimen was encapsulated in epoxy resin with an exposed surface with dimension of 10 mm×10 mm. The specimen surface was ground successively to 1 000 grit SiC paper. The hydrogen evolved during the immersion test was collected in a burette above the immersed specimen. The corrosion rates of the magnesium anodes were evaluated by measuring the volume of evolved hydrogen.

3 Results and discussion

3.1 Microstructure

Fig.1 shows the SEM images of Mg-6%Al-5%Pb and Mg-6%Al-5%Pb-0.55%Zn-0.22%Mn alloys. Their chemical compositions obtained by atomic absorption spectrum analysis are listed in Table 1. In this work, Mg-6%Al-5%Pb alloys are shown as alloy A while Mg-6%Al-5%Pb-0.55%Zn-0.22%Mn alloys are shown as alloy B. The microstructures of cast specimens of alloys A and B consist of the primary α-Mg grains and second phases distributed along the α-Mg grain boundaries. The distribution of the second phases is discontinuous. The microstructures of solid solution treatment and aged specimens of alloys A and B are homogeneous, but the volume fractions of the second phase particles of alloy B are larger than those of alloy A. The reason might be that after the addition of a small quantity of zinc and manganese in the magnesium matrix, the second phase particles are easy to precipitate in the magnesium matrix during the process of heat treatment.

3.2 Open circuit potential (OCP)

Fig.2 shows the evolution of the open circuit potentials (OCP) for alloys A and B in different heat treatment conditions immersed in 3.5% NaCl aqueous solution for 15 min. Each measurement started immediately after the specimen was immersed in NaCl aqueous solution. These curves reflect the initiation and propagation of corrosion. At the onset of corrosion there is an incubation period during which the OCP increases rapidly to the maximum value, indicating that an oxide film forms on the surface of the specimen. The subsequent decrease of the OCP indicates the breakdown of the oxide film with the effect of Cl^- ions in the electrolyte solution[9−10, 12, 18]. After the breakdown of the oxide film the OCP comes into steady state, indicating the dynamic balance between the advance of the corrosion and the deposit of the corrosion products. At steady state the whole specimen surface is corroded. It can be seen that the incubation periods of the specimens with the same composition but different heat treatment conditions are almost the same (Figs.2(a) and (b)), while the incubation periods of alloy B (approximately 200 s) under each heat treatment condition are shorter than those of alloy A (approximately 350 s) in the same condition (Figs.2(c)−(f)). It can also be seen that the OCP of alloy A in the steady state are more negative than that of alloy B under most heat treatment conditions except for the as-cast condition (Fig.2(f)). So, it can be concluded that the corrosion incubation period of the OCP of Mg-Al-Pb anode is mainly determined by its composition and it can be shortened with 0.55%Zn and 0.22%Mn additions in the magnesium matrix.

3.3 Potentiodynamic polarization curves

Fig.3 shows the potentiodynamic polarization curves

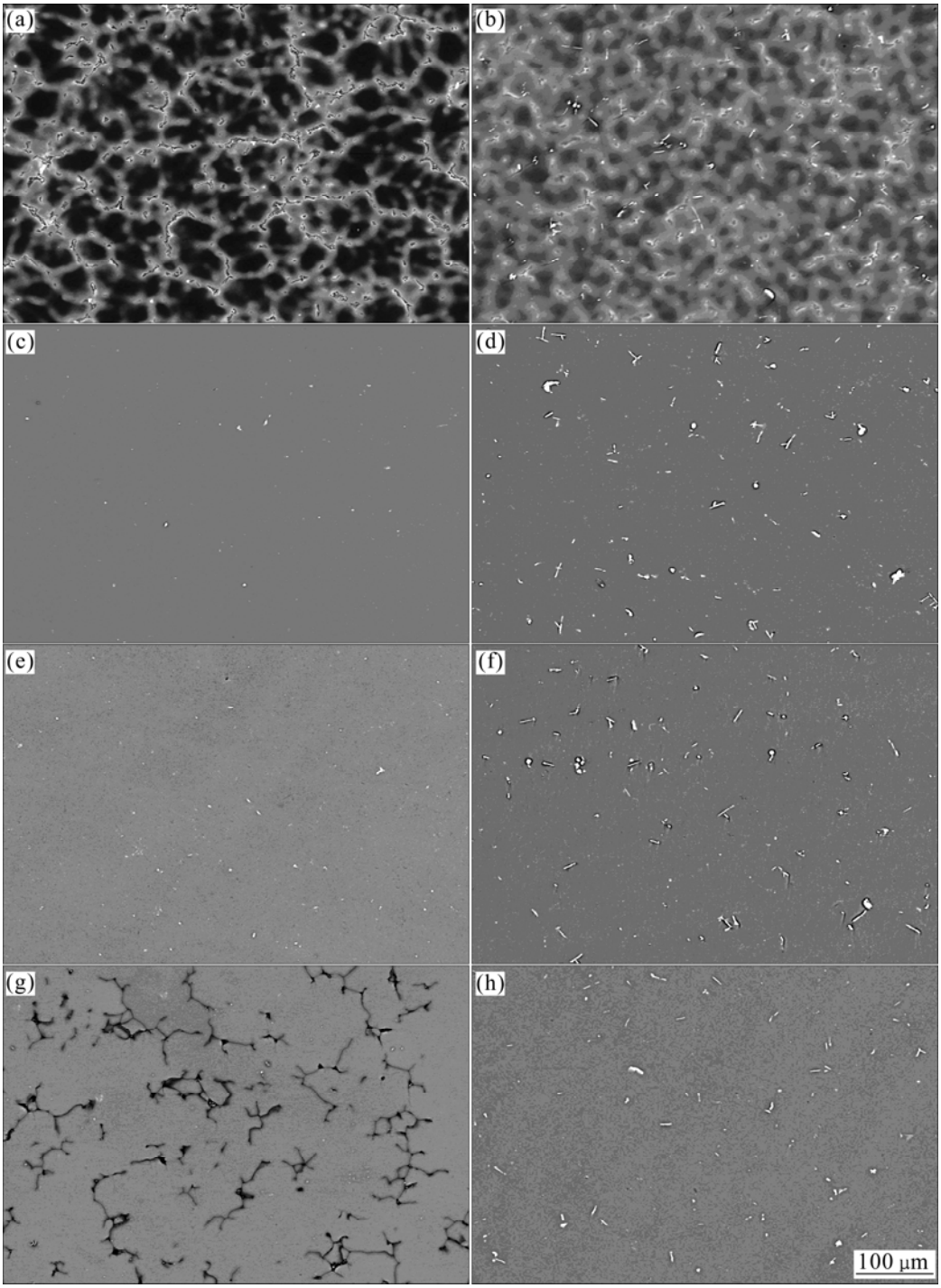

Fig.1 SEM images of alloys A and B in different heat treatment conditions: (a) Alloy A, as-cast; (b) Alloy B, as-cast; (c) Alloy A, solid solution treated; (d) Alloy B, solid solution treated; (e) Alloy A, aged at 200 ºC; (f) Alloy B, aged at 200 ºC; (g) Alloy A, aged at 100 ºC; (h) Alloy B, aged at 100 ºC

Table 1 Chemical compositions of alloys A and B (mass fraction, %)

Sample	Al	Pb	Zn	Mn	Fe	Ca	Cu	Sn	P	S	Mg
A	6.14	5.46	0.045	0.009	0.013	0.018	0.051	0.019	0.028	0.028	Bal.
B	6.11	5.17	0.561	0.216	0.009	0.013	0.004	0.001	0.019	0.007	Bal.

of alloys A and B under different heat treatment conditions immersed in 3.5% NaCl aqueous solution. Each measurement started immediately after the specimen was immersed in NaCl aqueous solution.

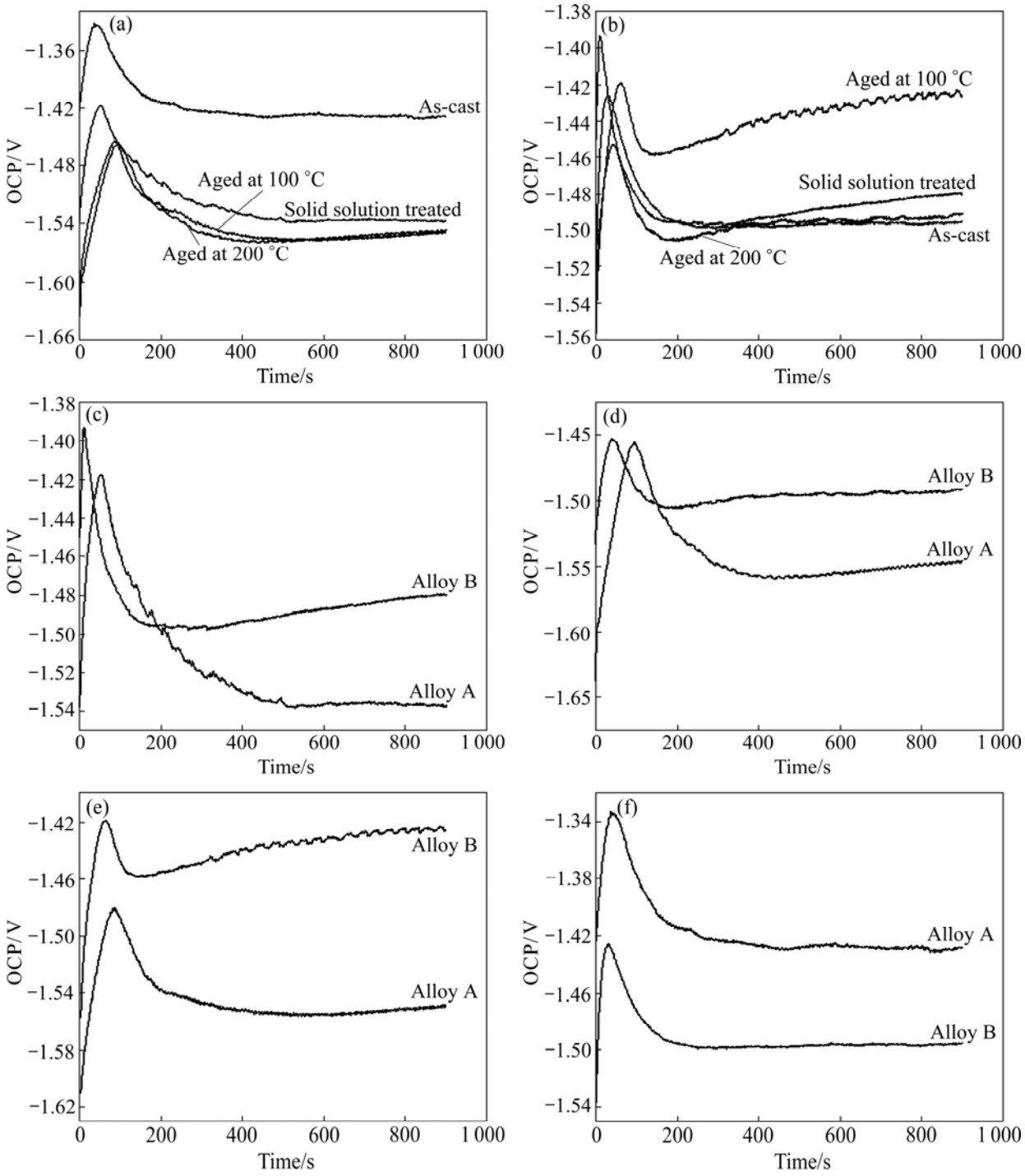

Fig.2 Evolution of open circuit potentials (OCP) of alloys A and B in 3.5% NaCl solution at 25 ºC: (a) Alloy A; (b) Alloy B; (c) Solid solution treated alloys; (d) Alloys aged at 200 ºC; (e) Alloys aged at 100 ºC; (f) As-cast alloys

These polarization curves were used to measure the corrosion current density J_{corr} at the corrosion potential φ_{corr} by Tafel extrapolation of the cathodic branch of the polarization curve. The polarization curves are not symmetrical in the anodic and cathodic branches. The rate of current increase in the anodic polarization branch is much greater than that in the cathodic branch. According to TAMAR and MANDLER[19], at more negative potentials than the corrosion potential (φ_{corr}), evolution of hydrogen dominates and results in cathodic current. At more positive potentials than φ_{corr}, magnesium oxidation dominates and the metal is continuously dissolved with the help of Cl^- ions, which can make the oxide film break down. It can be seen that the differences of the corrosion current densities (J_{corr}) among the specimens with the same composition but

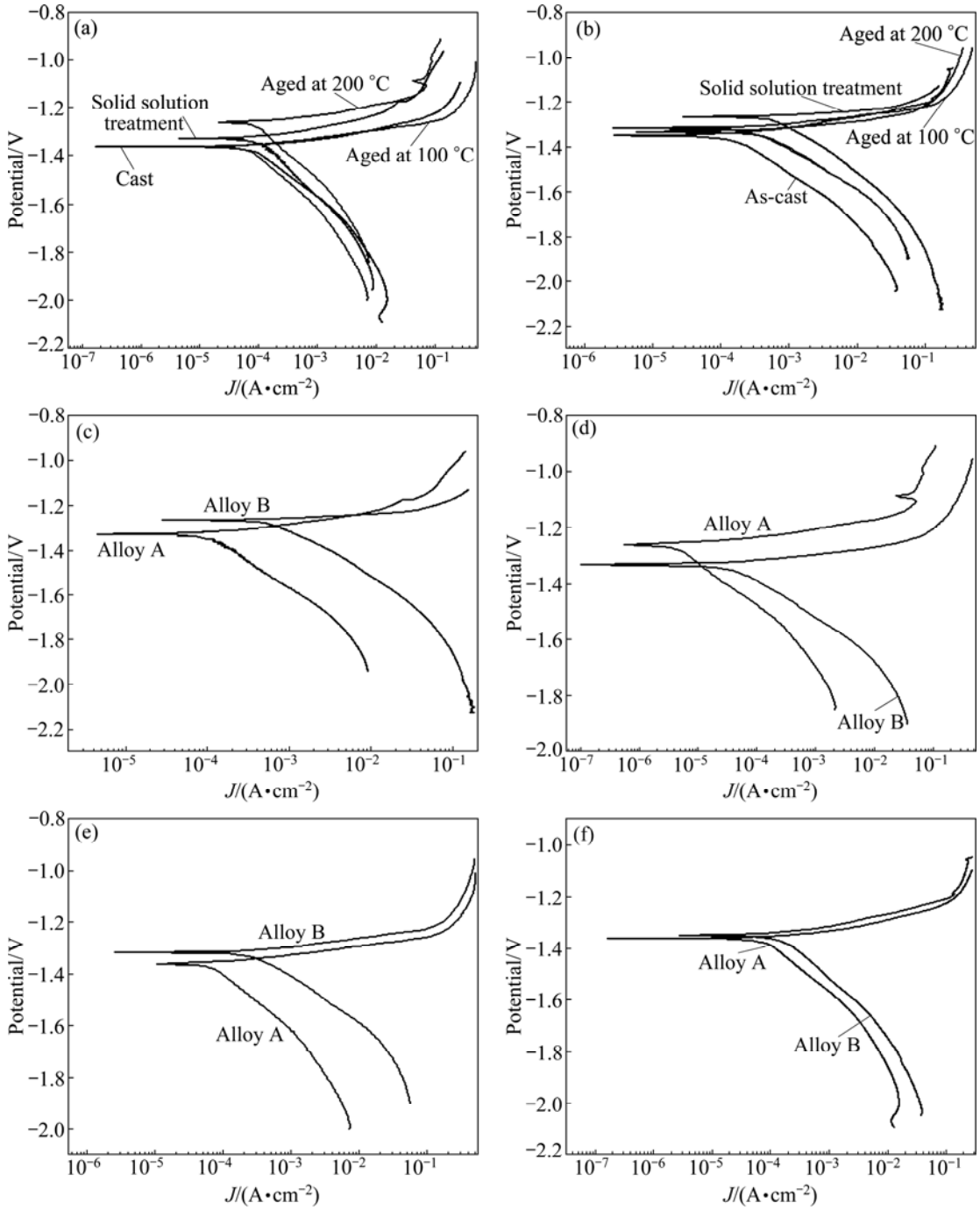

Fig.3 Potentiodynamic polarization curves of alloys A and B measured in 3.5% NaCl solution at 25 ºC: (a) Alloy A; (b) Alloy B; (c) Solid solution treated alloys; (d) Alloys aged at 200 ºC; (e) Alloys aged at 100 ºC; (f) As-cast alloys

different heat treatment conditions are not distinct (Figs.3(a) and (b)), while the corrosion current densities of alloy B in each heat treatment condition are higher than those of alloy A in the same condition (Figs.3(c)−(f)). The corrosion current densities (J_{corr}) and the corrosion potentials (φ_{corr}) of all these specimens are listed in Table 2.

According to ZHAO et al[9, 12], the corrosion current density is related to the average penetration rate, $P_{j\text{-Mg}}$ (mm/a), using

$$P_{j\text{-Mg}}=22.85J_{corr} \quad (1)$$

Table 3 lists the average penetration rate calculated using Eq.(1). It can be seen that the average penetration rate of solid solution treated alloy B is the highest while that of alloy A aged at 100 ºC is the lowest. The average penetration rate can be ranked in a decreasing series: alloy B, solid solution treated > alloy B, aged at 200 ºC > alloy B, aged at 100 ºC > alloy B, as-cast ≈ alloy A, as-cast ≈ alloy A, solid solution treated > alloy A, aged at 200 ºC ≈ alloy A, aged at 100 ºC. So, it can be concluded that

Table 2 Corrosion potentials (φ_{corr}) and corrosion current densities (J_{corr}) of alloys A and B under different heat treatment conditions

Sample	φ_{corr}/V	J_{corr}/(mA·cm^{-2})
Alloy A, as-cast	−1.336	0.121
Alloy A, solid solution treated	−1.328	0.116
Alloy A, aged at 200 ºC	−1.264	0.068
Alloy A, aged at 100 ºC	−1.359	0.063
Alloy B, as-cast	−1.295	0.164
Alloy B, solid solution treated	−1.266	0.794
Alloy B, aged at 200 ºC	−1.324	0.496
Alloy B, aged at 100 ºC	−1.321	0.251

Table 3 Average penetration rates of alloys A and B under different heat treatment conditions immersed in 3.5% NaCl solution

Specimen	$P_{H_2\text{-Mg}}$ / (mm·a^{-1})	$P_{j\text{-Mg}}$ / (mm·a^{-1})
Alloy A , as-cast	82.04	3.70
Alloy A, solid solution treated	84.23	2.65
Alloy A, aged at 200 ºC	60.17	1.55
Alloy A, aged at 100 ºC	44.30	1.44
Alloy B, as-cast	99.00	2.76
Alloy B, solid solution treated	148.23	18.14
Alloy B, aged at 200 ºC	84.78	11.33
Alloy B, aged at 100 ºC	88.61	5.74

the corrosion rate based on the corrosion current density of Mg-Al-Pb anode is mainly determined by its composition and it can be increased with 0.55%Zn and 0.22%Mn additions in the magnesium matrix. Besides, the corrosion rate might be related to the incubation period of the OCP mentioned above. Long incubation period always leads to low corrosion rate while short incubation period leads to high corrosion rate. But, the corrosion rate of Mg-Al-Pb anode is not determined by its OCP value, and more negative value of the OCP is not always correlated to higher corrosion rate. This is not consistent with what ZHAO et al[9] had reported about the corrosion behavior of ZE41 magnesium alloy in NaCl solution.

3.4 Hydrogen evolution

Fig.4 shows the hydrogen evolution volume

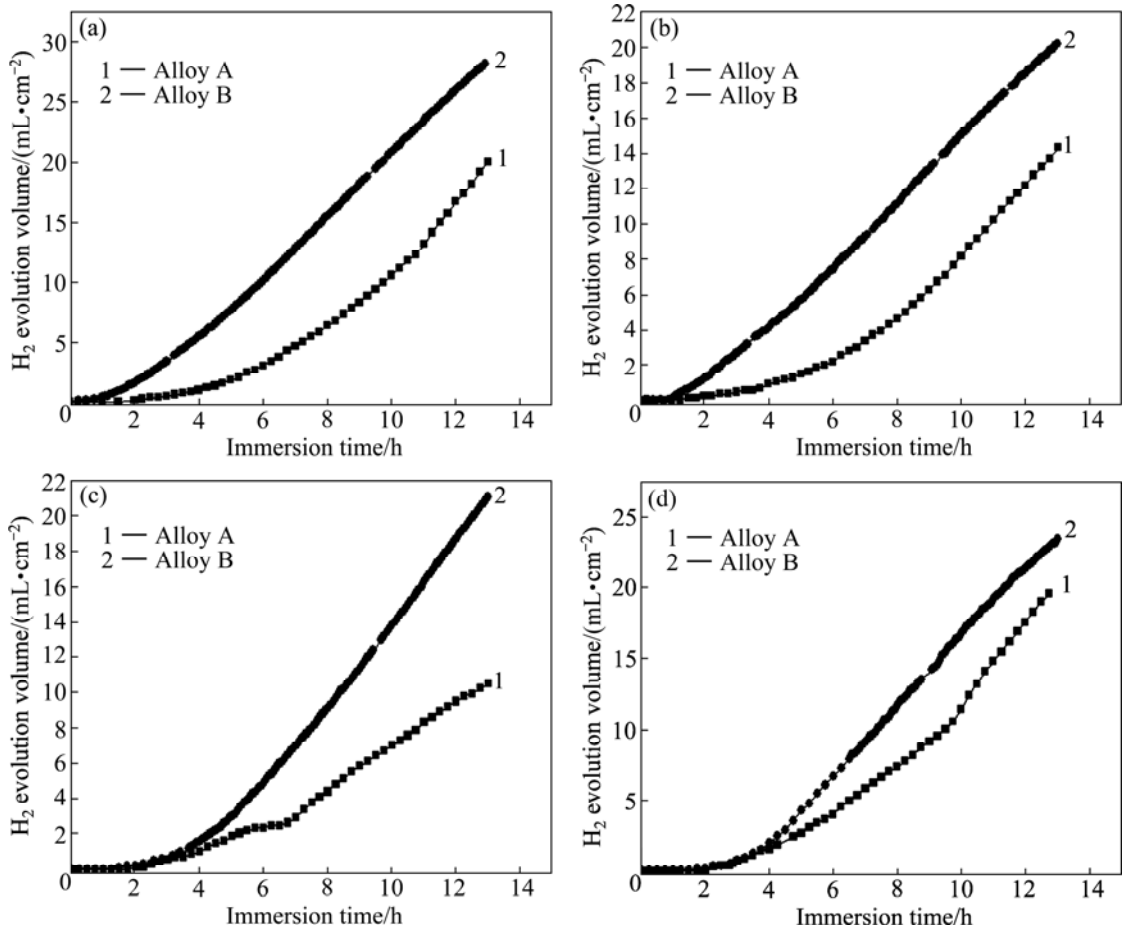

Fig.4 Hydrogen evolution volume as function of immersion time of alloys A and B immersed in 3.5% NaCl solution for 13 h: (a) Solid solution treated alloys; (b) Alloys aged at 200 ºC; (c) Alloys aged at 100 ºC; (d) As-cast alloys

(mL/cm^2), as a function of immersion time (h), of alloys A and B under different heat treatment conditions immersed in 3.5% NaCl aqueous solution for 13 h. It can be seen that there is initially an incubation period during which the rate of hydrogen evolution is quite low. The incubation periods of alloy B under each heat treatment condition are shorter than those of alloy A in the same condition, which is consistent with the incubation periods of the OCP mentioned above. Thereafter, the volume of hydrogen evolution increases with increasing immersion time, which can be attributed to the corrosion occurring on increasing corroded surface area of the specimen[12]. For long time immersion, the rate of hydrogen evolution becomes linear and the process of corrosion has achieved steady state. The incubation period of the hydrogen evolution is much longer than that of the OCP, indicating that the electrochemical technique is more sensitive in detecting the onset of corrosion than the technique based on the hydrogen evolution[9]. Fig.5 shows the volume of hydrogen evolution of alloys A and B under each heat treatment condition after being immersed in 3.5% NaCl solution for 13 h. It can be seen that the volume of hydrogen evolution of solid solution treated alloy B is the largest while that of alloy A aged at 100 ºC is the smallest. This is consistent with the average penetration rate $P_{j\text{-Mg}}$ (mm/a) obtained from the corrosion current density. The volume of hydrogen evolution can be ranked in a decreasing series: alloy B, solid solution treated > alloy B, as-cast > alloy B, aged at 100 ºC ≈ alloy B, aged at 200 ºC ≈ alloy A, solid solution treated ≈ alloy A, as-cast > alloy A, aged at 200 ºC > alloy A, aged at 100 ºC. This rank is similar to that of the average penetration rate obtained from the corrosion current density except for as-cast alloy B, and alloy B aged at 200 ºC. So, it can be concluded that the volume of hydrogen evolution of Mg-Al-Pb anode is mainly determined by its composition and it can be increased with 0.55% Zn and 0.22% Mn additions in the magnesium matrix.

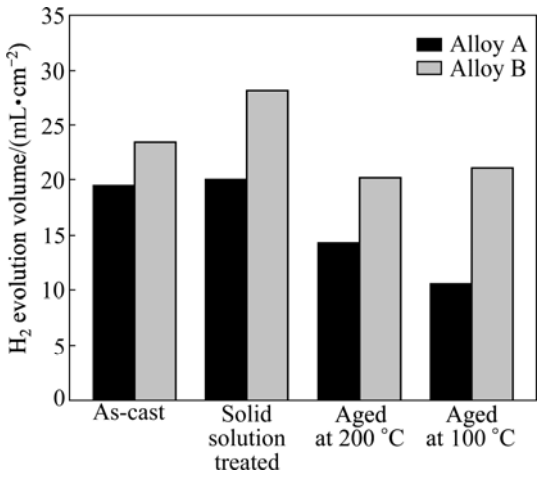

Fig.5 Volume of hydrogen evolution of alloys A and B immersed in 3.5% NaCl solution for 13 h

The average rate of hydrogen evolution, $v(H_2)$ (mL·cm^{-2}·h^{-1}), can be evaluated as

$$v(H_2)=V(H_2)/(St) \quad (2)$$

where $v(H_2)$ is the volume of hydrogen evolution (mL); S is the area of specimen surface (cm^2); t is the immersion time (h).

According to ZHAO et al[9, 12], the average rate of hydrogen evolution $v(H_2)$ is related to the average penetration rate ($P_{H_2\text{-Mg}}$ (mm/a)) using

$$P_{H_2\text{-Mg}} = 54.696\ v(H_2) \quad (3)$$

Table 3 lists the average penetration rate calculated using Eq.(1). It can be seen that the average penetration rate based on the corrosion current density at the free corrosion potential does not agree with the direct measurements evaluated from the evolved hydrogen and it is much higher when estimated from the hydrogen evolution rate. This is consistent with what ZHAO et al[9, 12] had reported about the corrosion behaviors of AZ31, AZ91, AM30, AM60 and ZE41 magnesium alloys in NaCl solution. The reason might be that the corrosion rate obtained from the corrosion current density may relate to the onset of corrosion, whereas the corrosion rate obtained from the hydrogen evolution relates to the corrosion for a long time after the corrosion onset, when the steady state is established and the corroded surface area is enlarged during the long-term immersion[9, 20].

4 Conclusions

1) There is an incubation period in the corrosion onset of Mg-Al-Pb anode. The incubation period is mainly determined by alloy composition, and it can be shortened with 0.55% Zn and 0.22% Mn additions in the magnesium matrix.

2) The corrosion rate of Mg-Al-Pb anode is mainly determined by the corrosion incubation period and short incubation period always leads to high corrosion rate while long incubation period leads to low corrosion rate. But the corrosion rate of Mg-Al-Pb anode is not determined by its OCP value, and more negative value of the OCP is not always correlated with the higher corrosion rate.

3) The electrochemical measurements of the corrosion rate, based on the corrosion current density at the corrosion potential, do not agree with the measurements evaluated from the evolved hydrogen volume.

References

[1] RENUKA R. Influence of allotropic modifications of surphur on the cell voltage in Mg-CuI(S) seawater activated batter [J]. Materials Chemistry and Physics, 1999, 59(1): 42−48.

[2] FENG Yan, WANG Ri-chu, YU Kun, PENG Chao-qun, LI Wen-xian. Influence of Ga and Hg on microstructure and electrochemical corrosion behavior of Mg alloy anode materials [J]. Transactions of Nonferrous Metals Society of China, 2007, 17(6): 1363−1366.

[3] RENUK A R. AgCl and Ag_2S as additives to CuI in Mg-CuI seawater activated batteries [J]. Journal of Applied Electrochemistry, 1997, 27(12): 1394−1397.

[4] CAO Dian-xue, WU Lin, WANG Gui-ling, LU Yan-zhou. Electrochemical oxidation behavior of Mg-Li-Al-Ce-Zn and Mg-Li-Al-Ce-Zn-Mn in sodium chloride solution [J]. Journal of Power Sources, 2008, 183(2): 799−804.

[5] FENG Yan, WANG Ri-chu, PENG Chao-qun, WANG Nai-guang. Influence of $Mg_{21}Ga_5Hg_3$ compound on electrochemical properties of Mg-5%Hg-5%Ga alloy [J]. Transactions of Nonferrous Metals Society of China, 2009, 19(1): 154−159.

[6] FIRA S S, KIBL L, LIW L W. Water-activated disposable and long shelf-life microbatteries [J]. Sensors and Actuators A, 2004, 111: 79−86.

[7] VENKATESARA R K. Performance evaluation of Mg-AgCl batteries for under water propulsion [J]. Defense Science Journal, 2001, 5(2): 161−170.

[8] FIDEL G M, JUAN M F, RUBEN D R, GENESCA J. Electrochemical study on magnesium anodes in NaCl and $CaSO_4$-$Mg(OH)_2$ aqueous solutions [J]. Electrochimic Acta, 2006, 51: 1820−1830.

[9] ZHAO Ming-chun, LIU Ming, SONG Guang-ling, ATRENS A. Influence of pH and chloride ion concentration on the corrosion of Mg alloy ZE41 [J]. Corrosion Science, 2008, 50: 3168−3178.

[10] HIROMOTO S, YAMAMOTO A, MARUYAMA N, SOMEKAWA H, MUKAI T. Influence of PH and flow on the polarization behaviour of pure magnesium in borate buffer solutions [J]. Corrosion Science, 2008, 50: 3561−3568.

[11] SHI Zhi-ming, SONG Guang-ling, ATRENS A. Influence of the β phase on the corrosion performance of anodised coatings on magnesium-aluminium alloys [J]. Corrosion Science, 2005, 47: 2760−2777.

[12] ZHAO Ming-chun, SCHMUTZ P, BRUNNER S, LIU Ming, SONG Guang-ling, ATRENS A. An exploratory study of the corrosion of Mg alloys during interrupted salt spray testing [J]. Corrosion Science, 2009, 51: 1277−1292.

[13] ZHAO Ming-chun, LIU Ming, SONG Guang-ling, ATRENS A. Influence of the β-phase morphology on the corrosion of the Mg alloy AZ91 [J]. Corrosion Science, 2008, 50: 1939−1953.

[14] GU Xue-nan, ZHENG Yu-feng, CHENG Yan, ZHONG Sheng-ping, XI Ting-fei. In vitro corrosion and biocompatibility of binary magnesium alloys [J]. Biomaterials, 2009, 30: 484−498.

[15] PARDO A, MERION M C, COY A E, VIEJO F, ARRABAL R, FELIUJR S. Influence of microstructrue and composition on the corrosion behaviour of Mg/Al alloys in chloride media [J]. Electrochimica Acta, 2008, 53: 7890−7902.

[16] CANDAN S, UNAL M, TURKMEN M, KOC E, TUREN Y, CANDAN E. Improvement of mechanical and corrosion properties of magnesium alloy by lead addition [J]. Materials Science and Engineering A, 2009, 501: 115−118.

[17] UDHAYAN R, BHATT D P. On the corrosion behavior of magnesium and its alloys using electrochemical techniques [J]. Journal of Power Sources, 1996, 63(1): 103−107.

[18] SONG Y W, SHAN D Y, HAN E H. Corrosion behaviors of electroless plating Ni-P coatings deposited on magnesium alloys in artificial sweat solution [J]. Electrochimica Acta, 2007, 53: 2009−2015.

[19] TAMAR Y, MANDLER D. Corrosion inhibition of magnesium by combined zirconia silica sol-gel films [J]. Electrochimica Acta, 2008, 53: 5118−5127.

[20] TAKENAKA T, ONO T, NARAZAKI Y, NAKA Y, KAWAKAMI M. Improvement of corrosion resistance of magnesium metal by rare earth elements [J]. Electrochimica Acta, 2007, 53: 117−121.

(Edited by LI Xiang-qun)